J. Astron. Space Sci. 15(2), 391–400 (1998)

ROCKET MEASUREMENT OF MIDDLE ATMOSPHERIC OZONE CONCENTRATION PROFILE BY KSR-II

Jhoon Kim[1], Soo Jin Lee[1], Hi-Ku Cho[2], Byoung Kwon Park[2], Jae Deuk Lee[1], Hyung-Don Choi[1], and Gwang Rae Cho[1]
[1]Korea Aerospace Research Institute(KARI), [2]Yonsei University
e-mail: jkim@kari.re.kr

(Received October 30, 1998; Accepted November 20, 1998)

ABSTRACT

KSR-II, a two-stage sounding rocket of KARI was launched successfully at the west coast of the Korean Peninsula at 1000LST, June 11, 1998. For the ozone measurement mission, 8-channel UV and visible radiometers were onboard the rocket. The rocket measured the first *in situ* stratospheric and mesospheric ozone density profile over Korea during its ascending phase using the radiometer. Comparisons with Dobson spectrophotometer, ozonesonde, and HALOE onboard the UARS are shown together. Our results are in reasonable agreements with others.

1. INTRODUCTION

The issue of ozone has attracted global concern since the discovery of ozone hole in 1985 (Farman *et al.* 1985). Satellites, rockets, balloons, and ground-based instruments have revealed the detail structure of the ozone distribution in spatial as well as temporal domain. Extensive efforts have been put to measure ozone concentration profiles using ground-based, balloons, rockets and satellites to date. Sounding rockets have played a significant role in measuring ozone concentration profiles of the intermediate altitudes where the balloons and satellites cannot reach for the precise *in situ* measurements. Korea Aerospace Research Institute (KARI) has flown four sounding rockets since 1993. KSR (Korea Sounding Rocket)-I series which was first launched in June 4, 1993 obtained two sounding data on stratospheric ozone concentration profiles (Kim *et al.* 1997) for the altitude range up to 45 km. KSR-II, a two-stage sounding rocket of KARI was launched successfully at the west coast of the Korean Peninsula at 1000LST, June 11, 1998. One of its scientific mission was to measure ozone density profile in the middle atmosphere. For this mission, 8-channel UV and visible radiometers were onboard the rocket. The apogee of the rocket was 137 km and the total flight time was 365 seconds, which provided excellent chance to obtain mesospheric ozone density profile as well as stratospheric one. The rocket measured the first *in situ* stratospheric and mesospheric ozone density profile over Korea during its ascending phase using the 8-channel radiometer and transmitted the data to ground station in real time (Figure 1). This paper reports the preliminary results of these measurements.

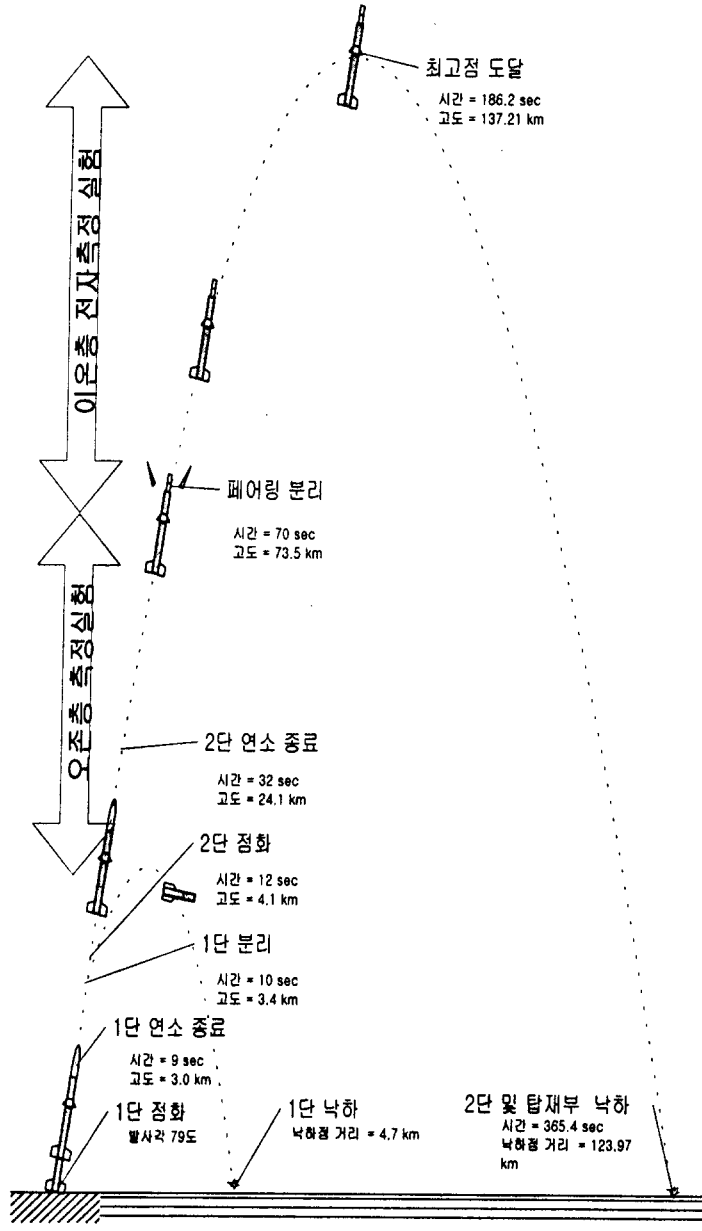

Figure 1. Trajectory of KSR-II with events.

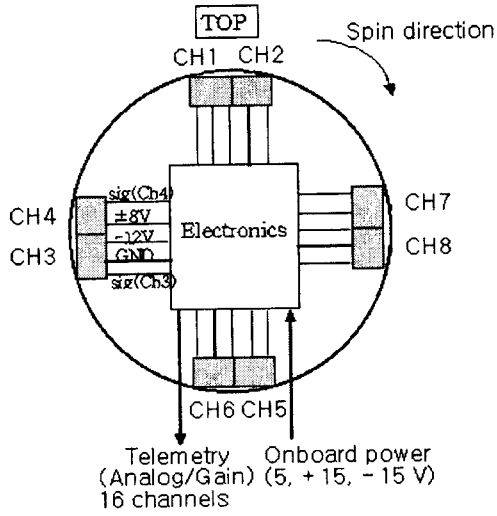

Figure 2. Ozone detector onboard the KSR-II.

2. INSTRUMENTATION

Ozone absorbs the solar UV radiation at Huggins and Hartley bands. This property is the important basis for the KSR ozone detector. One of the assumptions in the measurement is that the atmosphere is assumed to be uniform in horizontal direction for the solar zenith angle less than 60 deg. The current KSR ozone detecting system is a modified version of KSR-I's (Kim *et al.* 1997) which measures the attenuation of sunlight in ultraviolet absorption bands of ozone as a function of height with eight radiometers (see Figure 2). The number of radiometer channels has been doubled to compensate for the lower spin rate compared to the case of KSR-I. These radiometers were fixed on the rocket skin looking at an angle of 40 deg from the rocket body axis, to capture the Sun during the rocket flight within the FOV (field of view) of the detector considering the rocket trajectory, the predicted rocket attitude, and the position of the sun at the time and location of the launch. The ozone sensor consists of phototubes and interference filters to detect direct solar radiation at three UV and one visible wavelengths ($255 \pm 15, 290 \pm 15, 310 \pm 15$, and 450 ± 3 nm) during the ascending period of the rocket. This simple design provides FOV of about 50°. The incoming diffusive component of sunlight was assumed to be negligible compared to the total intensity measured by the instrument. One visible radiometer is for reference.

These radiometers use spin of the rocket to sweep the FOV past the solar disc. This captured solar radiation induces current from the phototube, which is then converted to analog voltage (0 – 5 V) in the circuit box. Analog output voltages and six-step gain levels for each radiometer channel were sampled at every 4 ms and telemetered in S band to the KARI's ground station. Ozone data are transmitted in a 16-channel, 10-bit pulse code modulation (PCM) system.

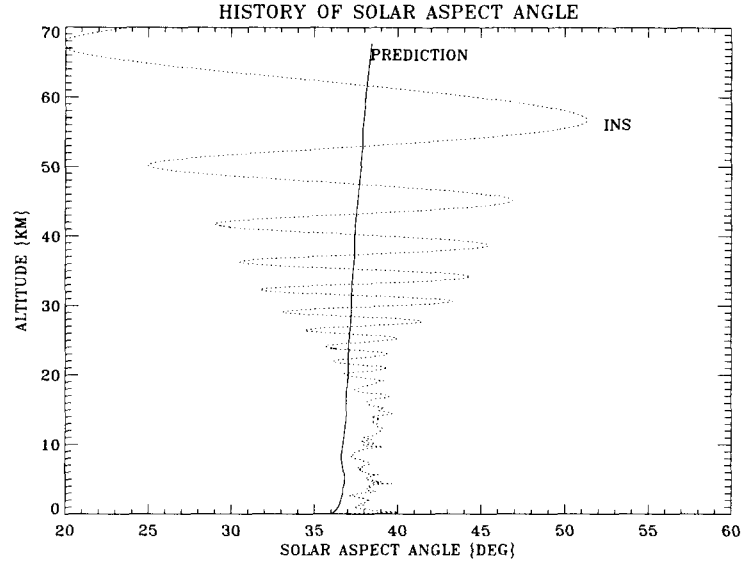

Figure 3. The comparison of predicted and INS-measured solar aspect angle during the flight.

As a redundant way to see the effect of solar aspect angle change, the angle was reduced from the onboard inertial navigation system (INS). Figure 3 shows the comparison between the calculated and measured values of the aspect angle during the flight. In general, the difference between the calculated and measured angles were within 2 deg up to 20 km due to active attitude control system by canard fins. These differences become larger as altitude increases due to nutational motion of the rocket, but still within the FOV of the detector up to 70 km. One can note that the incident angle change of the solar radiation on the detector is less than $\pm 20°$ up to 70 km, which is within the designed FOV of the detector.

3. DATA REDUCTION

In the data reduction algorithm, the atmosphere was assumed to be uniform in horizontal direction for the solar zenith angle less than 60 deg as shown in Figure 4. The average solar zenith angle for the current rocket measurement was 35.592 deg. One can utilize the larger optical path to obtain ozone measurements up to higher altitudes in the case with larger solar zenith angle close to 90 deg in the rocket measurements. For the case of solar zenith angle larger than 60 deg., the atmosphere cannot be assumed to be plane parallel due to the earth's curvature, where more sophisticated data reduction algorithm has to be considered (Kim *et al.* 1993). The geometry of the rocket measurement is shown in Figure 4. The atmosphere is divided into layers with thickness of 0.5 km, where the ozone concentration was assumed to be constant inside the layer. Figure 5 shows analog signals

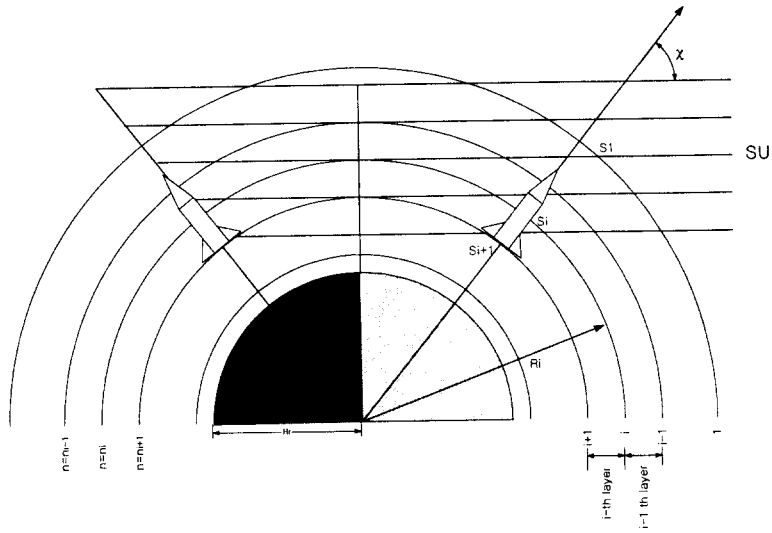

Figure 4. Geometry of rocket ozone measurement.

(in volts) as a function of flight time (in seconds) of the selected radiometer channels. The upper envelope of signals corresponds to ascending motion of the rocket, as shown in Figure 1 (KSR-II reached its apogee at t = 186 s). Thus these upper envelopes are expected to increase exponentially as the rocket passes the ozone layer and converged to a certain value after the rocket reached the top of the ozone layer, where the solar UV radiation at these wavelengths are no longer absorbed by ozone. Thus the oscillation of the upper envelope corresponds to the change of the rocket attitude, and the individual peak signals at $\sim$ 2.5-sec intervals are the result of changing solar radiation intensities during spinning motion of the rocket. Peak signals at 2.5-sec intervals were used to retrieve O_3 profiles with an altitude resolution of approximately 2.5 km. Note that the signals at shorter wavelengths (255 and 290 nm) responds at later time *i.e.* at higher altitudes compared to those of other longer wavelengths (310 and 450 nm) due to different absorption characteristics.

The relationship between the measured signal and ozone slant column density can be written as (Watanabe 1986)

$$\frac{I(z)}{I(z_o)} = \frac{\int_{\lambda_1}^{\lambda_2} F(\lambda)S(\lambda,\theta)\exp[-\sigma_a(\lambda,T(z))N(z) - \sigma_R(\lambda)M(z)]d\lambda}{\int_{\lambda_1}^{\lambda_2} F(\lambda)S(\lambda,\theta_o)\exp[-\sigma_a(\lambda,T(z_o))N(z_o) - \sigma_R(\lambda)M(z_o)]d\lambda} \tag{1}$$

where $I(z)$ is the measured intensity at altitude z, z_o is the highest altitude of the rocket measurements, $F(\lambda)$ is the solar flux at the top of the atmosphere as a function of wavelength, λ, $\sigma_a(\lambda, T(z))$ is the absorption cross section, $N(z)$ is the slant column ozone density above z, $T(z)$ is the temperature, $\sigma_R(\lambda)$ is the Rayleigh scattering coefficient, $M(z)$ is the slant air column density, $S(\lambda,\theta)$ is

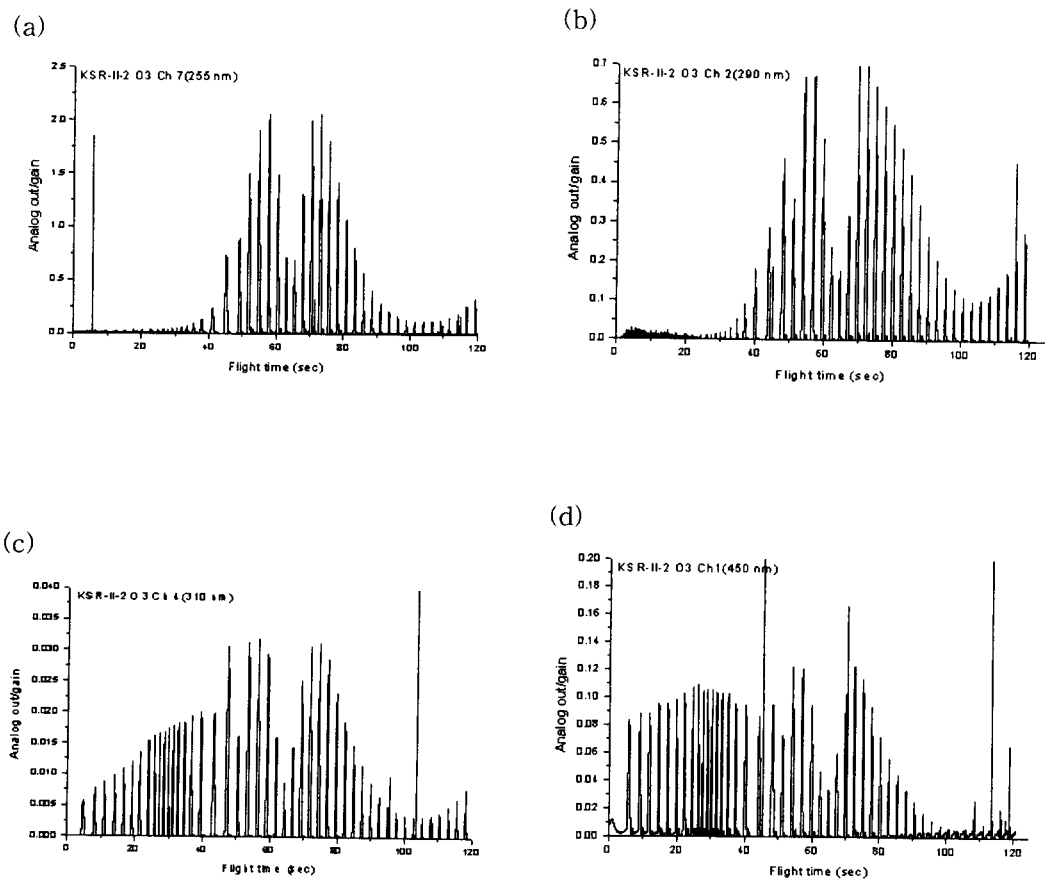

Figure 5. Signals of (a)255, (b)290, (c)310 and (d)450nm channel radiometers.

(a)

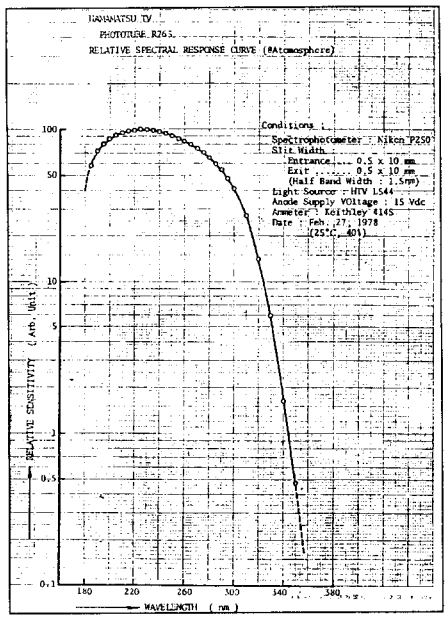

(b)

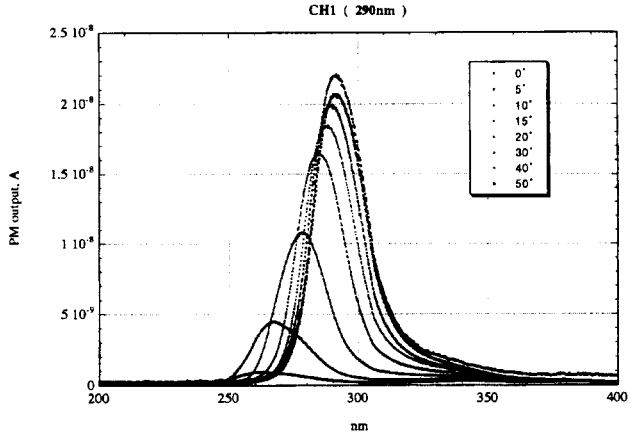

Figure 6. Response function of R765 phototube and 290 nm interference filter.

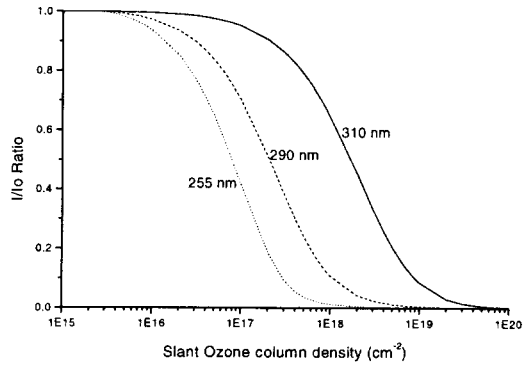

Figure 7. Relationship between ozone column density and the measured signal ratios at three wavelengths.

the response function of the radiometer measured in the laboratory, $S(\lambda, \theta) = S_{IF}(\lambda, \theta) S_{PT}(\lambda)$ where the subscript IF denotes interference filter, and PT denotes the phototube (Figure 6), and θ is the solar aspect angle, *i.e.* the angle between the sunlight and the radiometer pointing axis. The power of exponent in the denominator becomes to zero as $N(z_0)$ and $M(z_0)$ becomes zero over the ozone layer. Figure 6 shows the measured response function of the phototube, R765 and the interference filter at selected wavelength, 290 nm. Note that the center wavelength of the filter response function shifts to lower wavelengths and the transmittance function decreases as the incident angle changes from zero to 50 deg. The solar flux was taken from Mentall *et al.* (1981) and Thekaekara (1974). The absorption cross sections from Molina & Molina (1986) were linearly interpolated to the corresponding temperatures at different altitudes. The Rayleigh scattering cross sections were taken from WMO (1986). In this equation, Kim (1997) showed that the effect of Rayleigh scattering of the atmosphere is significant especially at lower altitudes less than 20 km. Figure 7 shows the relationship between the both sides of the eq. (1) for the three UV wavelengths and possible range of ozone column densities. The ozone number densities as a function of altitude can be obtained by differentiating the column densities obtained in the above process. Thus, the slope of the curves in Figure 7 provides information on the ozone measurements. As the curves converges to 1 as column densities decreases, the corresponding channel cannot distinguish the column density change. One can note that the 310 nm channel can be used in the larger ozone column densities, that is at lower altitudes, and 255 nm channel can be used in the smaller column densities, *i.e.* at higher altitudes. 290 nm channel can be used in the intermediate region.

4. RESULTS AND DISCUSSION

After the attitude correction of signals in Figure 5, the measured solar radiation intensities at selected wavelengths are obtained as a function of altitudes (see Figure 8). The increasing UV intensities at altitudes greater than 73 km is due to the very weak signals resulted from the attitude

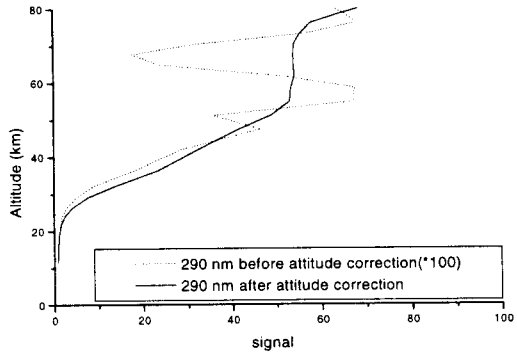

Figure 8. Comparisons of 290 nm signals before and after the attitude correction.

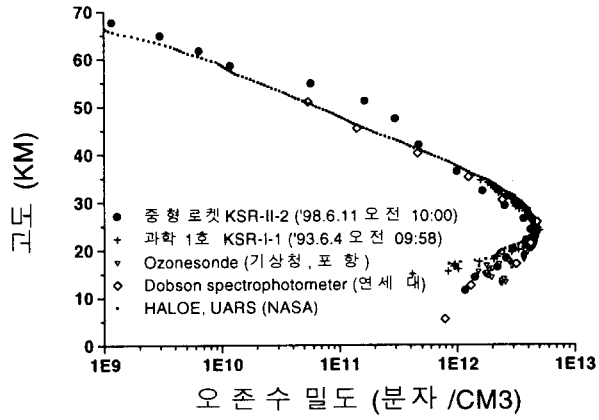

Figure 9. Retrieved ozone density profile. HALOE, Dobson spectrophotometer and balloon data are shown for comparison.

change of the rocket. Thus the ozone densities up to 70 km were obtained as shown in Figure 9. Comparisons with Dobson spectrophotometer, ozonesonde, and HALOE onboard the UARS are shown together. Our results are in reasonable agreements with others. The bulge of rocket measurement near 50 km is considered to be the effect of upward motion which can bring the ozone-rich atmosphere from the lower altitudes near the peak. Detail analysis using the comprehensive model needs to be carried out for this.

The ozone density profiles of different channels suggest that systematic error is very small in the measurements. The sources of errors in this rocket measurement include the error in characterizing filter response function, error in cross section data, error in attitude correction, telemetry and instrument noise, and error in estimating rocket altitude by radar. The largest uncertainties are due to the characterization of filter response function where the out-of-band filter response may cause nonnegligible errors. The errors in ozone density due to uncertainties in spectroscopic data are estimated to be less than 3% considering the accuracy and differences in the measurement of absorption cross section (*e.g.*, Molina & Molina 1986). The error in attitude correction was estimated to be about 2% for our case.

Random errors due to telemetry and instrument noise are estimated to be less than 2% for the current measurement. The rockets were tracked by radar at the ground. The error in rocket altitude is about 15 m based on the manufacturers specification. This error in determining rocket altitude can lead to less than 0.5% error in the O_3 density. Total random errors (1σ), estimated considering all sources discussed above, are 15% for the altitudes below 20 km, 7% for the altitude range between 20 and 50 km, and 10% for the altitude greater than 50 km.

ACKNOWLEDGEMENTS: Authors wishes to thank all participating people in the rocket development and launch. This research was supported by the Ministry of Science and Technology. The editor thanks two referees for their assistance in evaluating this paper.

REFERENCES

Farman, J. C., Gardiner, B. G., & Shanklin, J. D. 1985, Nature, 315, 207
Kim, J. 1997, JA&SS, 14, 87
Kim, J., Park, C. J., Lee, K. Y., Lee, D. H., Kim, Y. O., Cho, H. K., Cho, G. R., & Park, J. H. 1997, JGR, 102, 16121
Kim, J., Ryoo, J. S., Park, C. J., Lim, H. B., & Lee, K. Y. 1993, JA&SS, 9, 193
Mentall, J. E., Frederick, J. E., & Herman, J. R. 1981, JGR, 86, 9381
Molina, L. T. & Molina, M. J. 1986, JGR, 91, 14501
Thekaekara, M. P. 1974, Appl. Opt., 13, 518
Watanabe, T. 1986, Ph.D. Thesis, Tsukuba Univ.
WMO 1986, World Meteorological Organization Rep.16 (WMO: Washington D.C.), pp. 300